FORSCHUNGSZENTRUM
ROSSENDORF e.V.

FZR

FZR-107
September 1995
Preprint

S. Frauendorf, J. Reif and G. Winter

Shell-Model Study of Shears Bands in Light Pb Nuclei

Forschungszentrum Rossendorf e.V.
Postfach 51 01 19 · D-01314 Dresden
Bundesrepublik Deutschland

Telefon (0351) 591 3598
Telefax (0351) 591 3700
E-Mail reif@fz-rossendorf.de

Shell-Model Study of Shears Bands in Light Pb Nuclei

S. Frauendorf, J. Reif and G. Winter

Institut für Kern- und Hadronenphysik, Forschungszentrum Rossendorf, Postfach 510119, D-01314 Dresden, Germany

Abstract

Spherical shell-model calculations have been performed in the configuration space $(s_{1/2}h_{9/2}i_{13/2})$ and $(p_{1/2}p_{3/2}f_{5/2}i_{13/2})$ for protons and neutrons, respectively, in order to interpret the sequences of strong dipole transitions found in neutron-deficient Pb isotopes. Regular dipole bands are found if several high-j protons and high-j neutron holes are interacting with neutrons in the low-spin (fp) orbitals. The calculated $B(\mathrm{M1})$ values are in the order of several μ_N^2 for the ΔJ=1 transitions, and the crossover E2 transitions are very weak. The mechanism generating the dipole bands is found to be the same as in the TAC mean - field description.

1 Introduction

The low-lying states of the light Pb isotopes ($A < 208$) can be described as arising from spherical neutron configurations generated by the valence holes in the N=126 shell maintaining the closed Z=82 proton shell. The high-spin isomeric states can be interpreted as particle-hole excitations of the broken proton and $i_{13/2}$ neutron holes in stretched coupling. This body of irregularely spaced levels fits very well with the standard concept that semi-magic nuclei are nearly spherical. The discovery of very regular rotational bands at high spin in both even and odd Pb nuclei [1,2] (for the subsequent work see [3,4] and the references therein) has been quite a surprise. The characteristics of these bands are rather unusual. The sequence always starts at angular momenta larger than 10. The levels are linked by strong magnetic dipole transitions ($\Delta J = 1$), with $B(\mathrm{M1})$ values being in the order of several Weisskopf units. If observed at all, the crossover $\Delta J = 2$ transitions are very small, with $B(\mathrm{E2})$ values corresponding to $(Q_t < (1eb)^2)$. On the other hand, these bands are characterized by substantial dynamical moments if inertia ($\mathcal{J}^{(2)} \approx 15...25\mathrm{MeV}^{-1}$), which is about one half of the moment of inertia of well deformed nuclei. The ratio $\mathcal{J}^{(2)}/B(E2)$ is about 150 $\mathrm{MeV}^{-1}(eb)^{-2}$ to be compared to 15 $\mathrm{MeV}^{-1}(eb)^{-2}$ in well deformed and 5 $\mathrm{MeV}^{-1}(eb)^{-2}$ in superdeformed nuclei. In brief, one observes *very regular* $\Delta J = 1$ *bands in almost spherical nuclei* !

Preprint submitted to Elsevier Science *5 September 1995*

A first analysis of the structure of the dipole bands has been carried out in Refs. [1,3,5]. A break-up of the proton Z=82 shell is assumed, the protons being excited to high-j orbitals (e.g. $h_{9/2}$ or/and $i_{13/2}$) across the shell gap. The protons occupying high-K states induce a slight oblate deformation ($\epsilon_2 \approx$ -0.1). These protons are coupled to neutron holes in the intruder orbital $i_{13/2}$, which carry angular momentum aligned with the collective rotational axis. The regular rotation is assumed to be similar to the collective rotation in high-K bands of well deformed nuclei.

Though essential aspects of the structure of the dipole bands are accounted for by this interpretation, there are several problems. The assumed collective rotation of high-K intrinsic states is only justified for sufficiently large deformation. The most unusual feature of the bands remains unexplained: How can a nucleus with such a tiny deformation develop long regular rotational bands with a large moment of inertia? The explanation has been given within the tilted axis cranking (TAC) approach [6]. It is illustrated in Fig. 1. The $h_{9/2}$ and $i_{13/2}$ protons, have a torus like density distribution and the $i_{13/2}$ neutron holes a dumb-bell like one. At the band head the proton angular momentum is parallel to the symmetry axis and the neutron one perpendicular to it. In this way the overlap is maximized and the energy minimized. Along the band, both the angular momentum and the energy increase due to a gradual alignment of the proton and neutron spin into the direction of the total angular momentum. As this mechanism reminds of the closing of the blades of a pair of shears the name "shears bands" has been suggested in Ref. [3]. Most of the dynamical moment of inertia $\mathcal{J}^{(2)}$ is generated by this shears mechanism, which permits a regular rotational level spacing in spite of a very small deformation. The TAC calculations for the isotopes $^{197-202}$Pb [6,3,9] reproduce fairly well the experimental routhians, angular momenta and momenta of inertia of the regular sequences. The observed large B(M1) values and very small B(E2) values are also given by the TAC model [7]. The calculated deformations are always small ($\beta = 0.05...0.1, \gamma \approx -60°$) resulting in only a minor contribution of the collective rotation to $\mathcal{J}^{(2)}$.

In this paper we try to describe the dipole bands in terms of the spherical shell model. There are two reasons for such a study. On the one hand the possibility to obtain long regular rotational sequences as a result of a diagonalization of a spherical shell-model hamiltonian, is quite a theoretical challenge. The small deformations found in the TAC mean - field calculations seem to promise that it is possible to remain within a manageable configuration space. On the other hand, fast M1 transitions occur in many nuclei in the vicinity of closed shells [10], which have been interpreted successfully within the shell model [11]. In general these sequences are not characterized by regular level spacings but show a multiplet-like level ordering. The shell model is expected to disclose the relation between these "irregular" dipole sequences and the "regular" shears bands and should provide information about the origin of the regularity of

the latter. Both regular and irregular sequences have been observed in the Pb isotopes. A preliminary report of the present study has been given in Ref. [12].

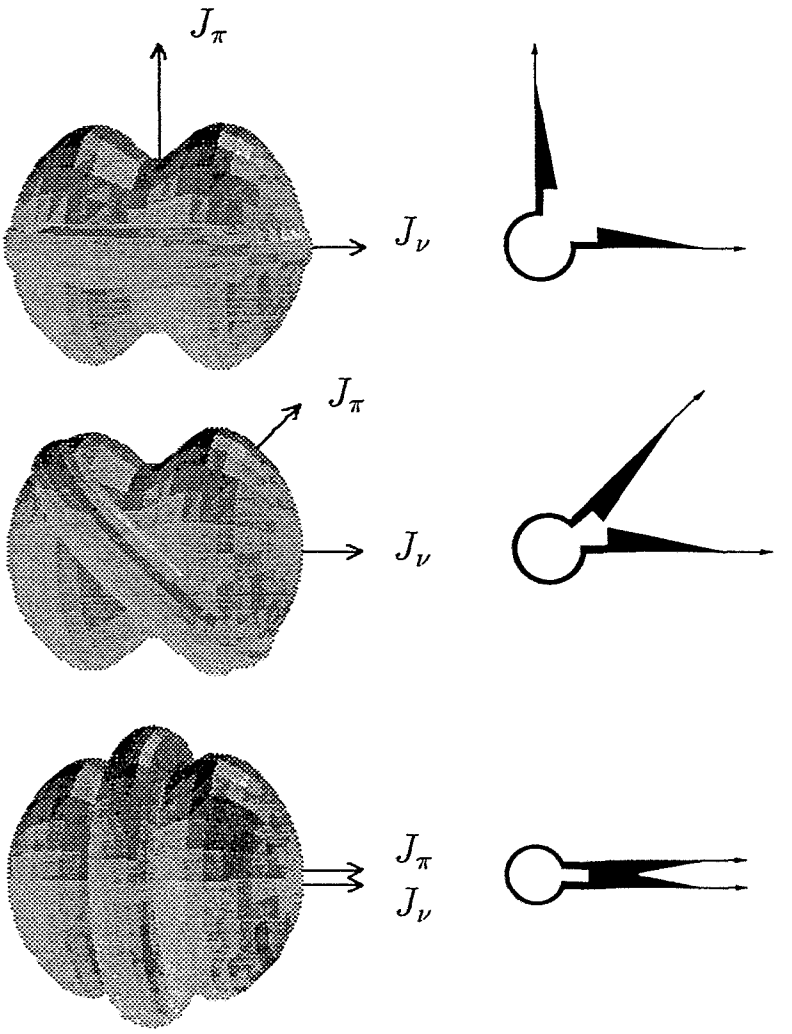

Fig. 1. Schematical representation of the density distribution of the high-j proton particles (torus like) and neutron holes (dumb-bell like) in a shears band. From the top to the bottom, the three panels correspond to the beginning, the middle and the end of the band.

2 The shell-model calculations

The calculations have been performed in the configuration space generated from the proton (π) $s_{1/2}$,$h_{9/2}$,$i_{13/2}$ and the neutron (ν) $p_{1/2}$,$p_{3/2}$,$f_{5/2}$,$i_{13/2}$ orbitals using the code RITSSCHIL [13]. In order to keep the computational

effort within reasonable limits the following restrictions have been made. In the proton system only the stretched configurations $(s_{1/2}^{-1}h_{9/2})_{5^-}$, $(s_{1/2}^{-2}h_{9/2}^{2})_{8^+}$, $(s_{1/2}^{-2}h_{9/2}i_{13/2})_{11^-}$ have been considered, whereas for the neutrons the configurations $[(p_{1/2}p_{3/2}f_{5/2})^{-m}(i_{13/2})^{-n}]$ with $m = 0, ..., 12$ and $n = 0, 1, 2$ have been taken into account. In the following we denote by "(fp) space" the configurations generated by neutrons in the $p_{1/2}$,$p_{3/2}$,$f_{5/2}$ orbitals. For the single-particle energies the experimental values with respect to the ^{208}Pb core have been taken [14]. The residual interaction has been approximated by the surface delta interaction [15]. The strength parameter of the isoscalar part ($A_{T=1}$ =0.32MeV) has been adjusted to the spherical spectra of the even $^{198-206}$Pb isotopes taking into account neutron excitations in the (fp) space only (see Fig. 2). Using this strength parameter the calculated energies of the considered high-j proton pair are in fair agreement with the experimental observations, as shown in Fig. 3.

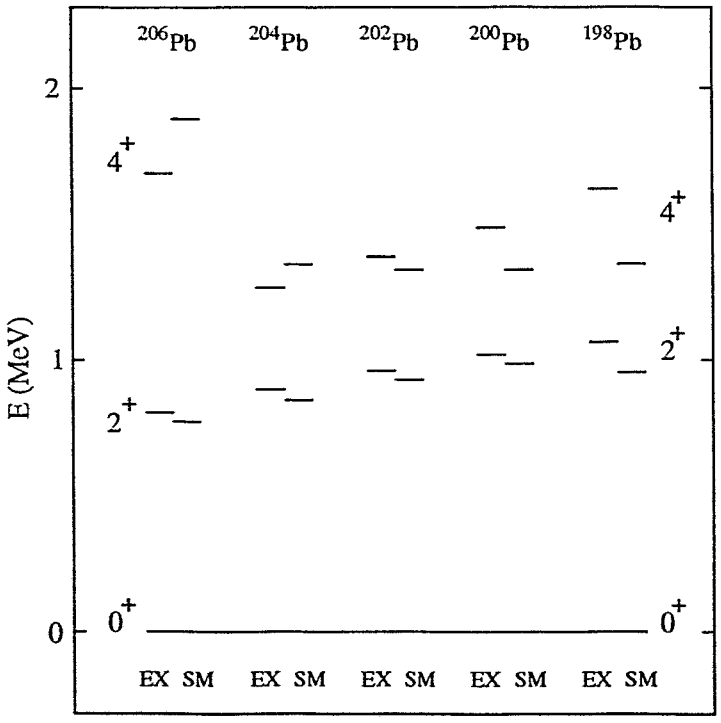

Fig. 2. Comparison of experimental (EX) and calculated (SM) lowest-lying 2^+ and 4^+ states in $^{198-206}$Pb. The shell-model calculation includes only neutron-hole excitations in the $p_{1/2}$,$p_{3/2}$,$f_{5/2}$ orbitals.

The $T = 0$ component of the proton-neutron interaction has been calculated with the same value of the strength parameter as the neutron-neutron and proton-proton interaction ($A_{T=1} = A_{T=0} = 0.32$MeV). Moderate variations of the interaction strength turned out to change only slightly the results given

below. For calculating electromagnetic transition probabilities the effective charges $e_\pi = 1.96e$, $e_\nu = 0.96e$ [16] and the effective g factors $g_s^{eff} = 0.7 g_s^{free}$ have been applied, which give a good description of the spherical shell model states.

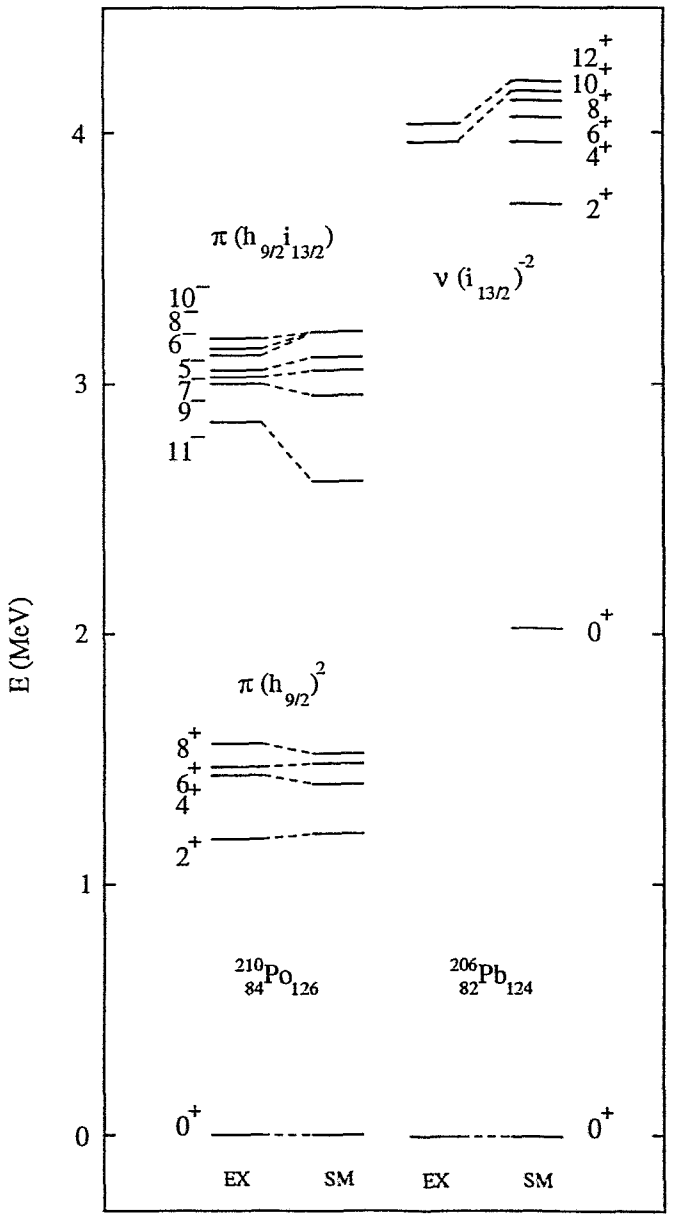

Fig. 3. Comparison of experimental (EX) and calculated (SM) states in ^{210}Po and ^{206}Pb assigned to the $\pi(h_{9/2})^2$, $\pi(h_{9/2}i_{13/2})$ and $\nu(i_{13/2})^{-2}$ configurations, respectively. The shell-model calculation includes only proton-particle excitations in the $h_{9/2}$,$i_{13/2}$ orbitals and neutron-hole excitations in the $i_{13/2}$ orbital, respectively.

3 The multiplet configurations

Fig. 3 shows the calculated energies of the neutron $(i_{13/2})^{-2}_{J+}$ and proton $(s^{-2}_{1/2}h^{2}_{9/2})_{J+}$ and $(s^{-2}_{1/2}h_{9/2}i_{13/2})_{J-}$ multiplets. Though the states with an angular momentum difference $\Delta J = 1$ are connected by strong magnetic transitions, they do not form a regular band. The calculation does also not give regular band structures if the neutron configuration $(i_{13/2})^{-2}_{12+}$ or the proton configurations $(s^{-1}_{1/2}h_{9/2})_{5-}$, $(s^{-2}_{1/2}h^{2}_{9/2})_{8+}$, $(s^{-2}_{1/2}h_{9/2}i_{13/2})_{11-}$ are coupled to several low-j neutrons in the (fp) space. This reflects the fact that in the semi-magic Pb isotopes the deformation induced by the valence nucleons is much too small to allow for collective rotation. In experiment [3,4] no band structures have been found built on the corresponding $8^+, 11^-$ and 12^+ isomeric states.

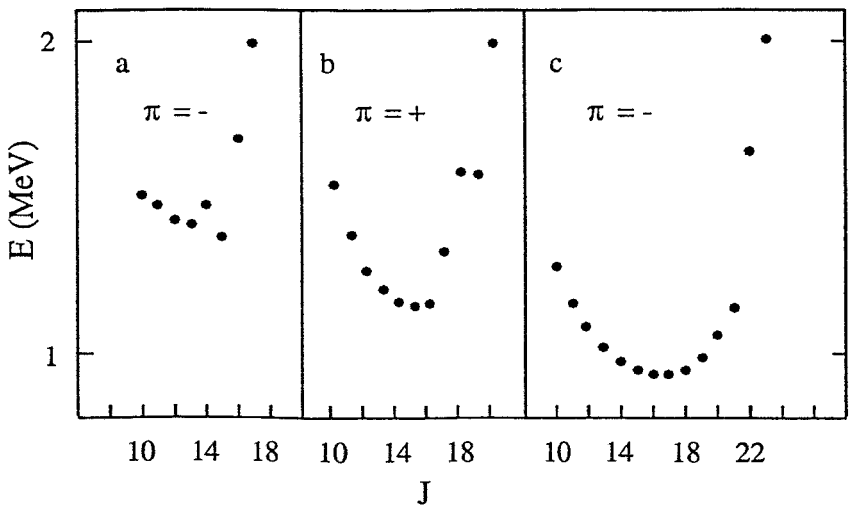

Fig. 4. Calculated excitation energy of states with $J \geq 10$ built by the coupling of the fully aligned neutron $(i_{13/2})^{-2}_{12+}$ configuration to the proton $(s^{-1}_{1/2}h_{9/2})_{5-}$ (a), $(s^{-2}_{1/2}h^{2}_{9/2})_{8+}$ (b) and $(s^{-2}_{1/2}h_{9/2}i_{13/2})_{11-}$ (c) excitations. The energies are normalized to the energy of the state with the highest spin.

In Ref. [6] it has been pointed out that only the combination of the mentioned proton configurations with $(i_{13/2})^{-n}$ neutron configurations to a "pair of shears" can generate a regular band. In order to investigate this idea closer, we start by coupling the fully aligned neutron $(i_{13/2})^{-2}_{12+}$ configuration and the considered fully aligned proton configurations to the total spin J. In Fig. 4 the energy of the states with $J \geq 10$ is shown as a function of the spin. Minimal energy is obtained for the perpendicular coupling of the proton particles to the neutron holes, since there is maximal overlap between the torus like density distribution of the protons and the dumb-bell like density distribution of the neutron holes. The alignment of the two spins into the direction of the total angular momentum leads to an increase of the energy, since the overlap

is reduced (cf. Fig. 1). This "restoring force" that tries to keep the blades of the shears open can clearly be recognized in Fig. 4.

The 11^- state represents the energetically lowest level of the $(h_{9/2}i_{13/2})$ multiplet and the restriction to the stretched configuration seems to be justified. In the $(s^{-2}_{1/2}h^2_{9/2})_{8+}$ proton multiplet the stretched configuration is not favored as compared to the nonstretched ones. This implies that sequences of states based on the proton configurations $(s^{-1}_{1/2}h_{9/2})_{5-}$ and $(s^{-2}_{1/2}h^2_{9/2})_{8+}$ should be less regular. The experiments in Ref. [3,4] seem to be in accordance with this observation. In the present paper we are mainly interested in the origin of the amazing regularity of the "shears bands". Accordingly, we will only consider the most favorable proton configuration $(s^{-2}_{1/2}h_{9/2}i_{13/2})_{11-}$ in the following.

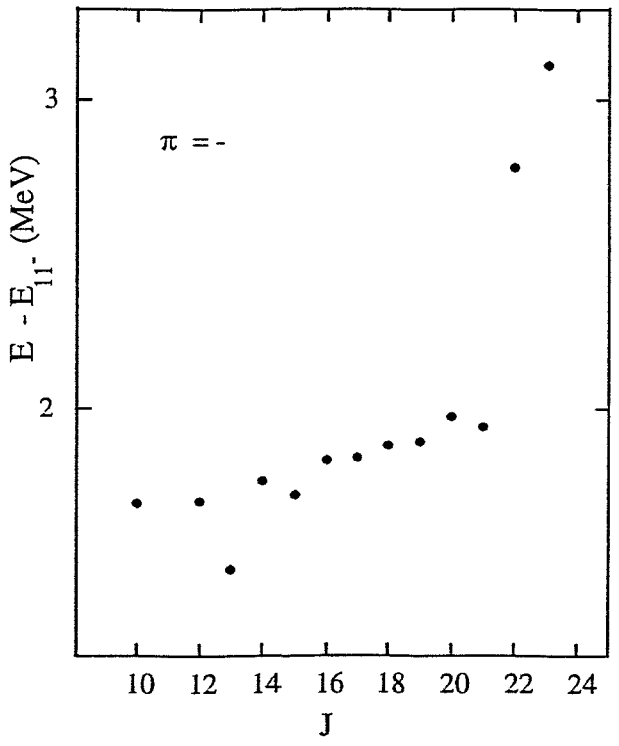

Fig. 5. Calculated excitation energy of the yrast states with $J \geq 10$ generated by the coupling of two holes in the neutron $i_{13/2}$ orbital to the proton $(s^{-2}_{1/2}h_{9/2}i_{13/2})_{11-}$ configurations. The energies are normalized to the energy of the 11^- state (not shown in the figure) which has the lowest energy due to the coupling of the paired $(i_{13/2})^{-2}_{0+}$ neutron configuration to the considered proton excitation.

The stretched 12^+ neutron configuration is energetically unfavored as compared to the other states of the $(i_{13/2})^{-2}$ multiplet. Thus, it is not obvious that there can exist a band in which the two neutron holes stay fully aligned with respect to each other. In order to study this question, we lift the limita-

tion to the parallel coupling of the two $i_{13/2}$ neutron holes. The result of the configuration mixing in the space $\pi(s_{1/2}^{-2}h_{9/2}i_{13/2})_{11^-} \otimes \nu(i_{13/2}^{-2})$ is illustrated in Fig. 5, which shows the energy of the lowest level for each state with $J \geq 10$. In comparison with Fig. 4c the function $E(J)$ does neither exhibit a minimum for spin $J \approx 17$ nor a smooth increase for the higher spins. These features can be understood by analyzing the calculated wave functions. The states with $10 \leq J \leq 15$ are mainly built from neutron excitations of low spin ($J = 0, 2, 4$), which have low excitation energies. These states correspond to spherical configurations and are not of relevance for the shears bands. The states with $J \geq 15$ include more and more the high-spin members of the neutron $(i_{13/2})^{-2}_{J_\nu}$ multiplet ($J_\nu = 6, 8, 10, 12$), which differ only little in energy. As seen in Fig. 4c, the states with the highest spins have energies similar to ones of the stretched configuration. This is expected, because the coupling of the neutron holes must be nearly stretched to generate the spin. For lower spins the nonstretched couplings of the neutron hole pair come into play, generating irregularities. For the spins near and above 15, the calculation represents two counteracting effects. The proton - neutron interaction favors the aligned coupling of the two neutron holes (cf. the overlap argument discussed in connection with Figs. 1 and 4). The neutron - neutron interaction favors the low J members of the neutron hole pair (cf. Fig. 3). The energies are comparable and an irregular behavior results from the competition. Hence, coupling a pair of nonequivalent high-j protons with a pair of equivalent high-j neutrons results in a sequence of irregularely spaced levels that are connected by strong magnetic transitions.

4 Appearance of bands

From previous steps it has become clear that there must be an additional mechanism that favors the fully aligned neutron $(i_{13/2})^{-2}_{12^+}$ configuration. To speak pictorially, one needs some "glue" that fixes the two $i_{13/2}$ neutron holes into "one stiff blade of the shears". This may be achieved by putting neutrons into $p_{1/2}$,$p_{3/2}$,$f_{5/2}$ orbitals. Such an open shell system is known to show a high quadrupole polarizability (cf. Ref. [17] and Ref. [18,11] in the context of shell-model calculations). The polarization modifies the interaction between the high-j orbitals in such a way that the aligned coupling of the $i_{13/2}$ neutron holes becomes stabilized.

The results of the calculations where the configuration space has been expanded by the neutrons in the (fp) space are summarized in Figs. 6 and 7, which show the spin J as a function of the energy difference between adjacent yrast states with J and $J-1$ (rotational frequency ω). Such a plot magnifies the irregularities. The level spacings are irregular if the (fp) shell is empty or full. The inspection of the wave functions reveals that this irregularity is ac-

companied by changes of the orientation of the two $i_{13/2}$ neutron holes relative to each other. Regular spacings appear only in the middle of the (fp) shell ($m \approx 3-7$), where the two $i_{13/2}$ neutron holes are predominantly coupled to $J_{i_{13/2}} = 12$. A gradual transition of the function $J(\omega)$ from irregular to regular and back to irregular is observed when filling the (fp) space. Hence, the neutrons occupying the (fp) shell cause the fully aligned coupling of the two neutron $i_{13/2}$ holes making the the regular shears bands to appear.

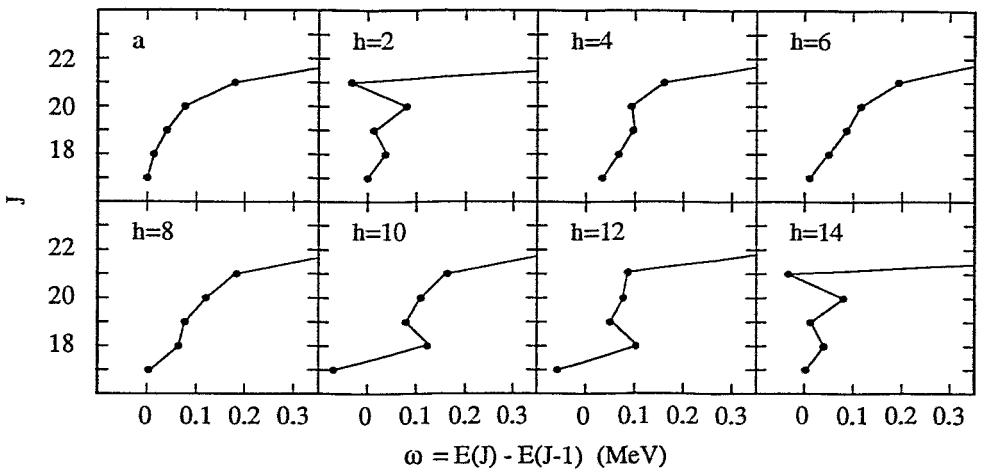

Fig. 6. Calculated dependence of the angular momentum J ($17^- \leq J^\pi \leq 22^-$) on the frequency ω. In the calculation the coupling of the proton $(s_{1/2}^{-2}h_{9/2}i_{13/2})_{11^-}$ excitation to the neutron configurations $(i_{13/2})^{-2}_{12^+}$ (a) and $(i_{13/2})^{-n}(p_{1/2}p_{3/2}f_{5/2})^{-m}$ (n=0,2; m even; $h = m + n$ denotes the total number of neutron holes) has been considered.

The details are as follows. The wave function of the (fp) neutrons is mainly composed of states with $J_{(\mathrm{fp})} = 0, 2, 4$, which may combine to a slightly deformed density distribution. The shape of the distribution is induced by the high-j particles. A feedback mechanism is active between the neutrons in the low- and and the nucleons in the high-j orbitals: The dumb-bell like density distribution of the $i_{13/2}$ holes induces a prolate deformation of the (fp) density and the prolate (fp) density aligns the $i_{13/2}$ holes. As a result, the aligned coupling of the high-j neutrons is stabilized. The analogue feedback is active between the high-j proton pair and the (fp) neutrons. The proton density distribution is torus like. It induces an oblate deformation of the (fp) neutron density, which stabilizes the aligned coupling of the proton pair as well as the aligned coupling of the $i_{13/2}$ neutron holes. The actual density distribution of the (fp) neutrons is a compromise between the driving forces of the high-j neutrons and protons. We have not calculated it. Probably it is triaxial-oblate, because oblate shape is still favored by the neutrons (cf. Fig.

1). If the (fp) space is half filled, the feedback resulting from the combined neutron and proton polarization is strong enough to keep the $i_{13/2}$ neutron hole pair aligned. Its spin can take many different orientations with respect to the proton spin, like in the case when we considered the coupling of the stretched proton to the stretched neutron configuration (Fig. 4c). A regular shears band is formed.

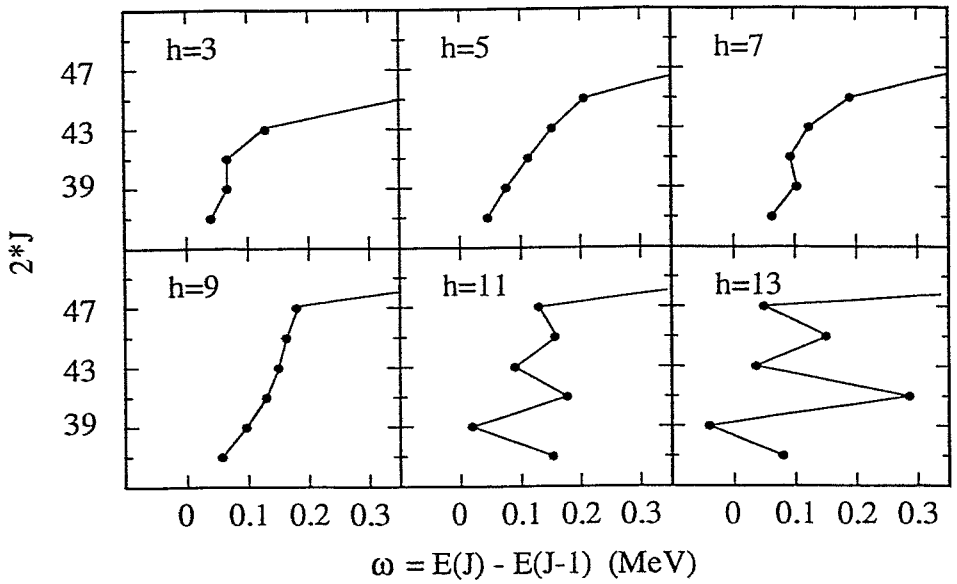

Fig. 7. Calculated dependence of the angular momentum J ($37/2^+ \leq J^\pi \leq 49/2^+$) on the frequency ω. In the calculation the coupling of the proton $(s_{1/2}^{-2}h_{9/2}i_{13/2})_{11}$-excitation to the neutron configurations $(i_{13/2})^{-n}(p_{1/2}p_{3/2}f_{5/2})^{-m}$ (n=0,2; m odd, $h = m + n$ denotes the total number of neutron holes) has been considered.

In brief, the regular level spacings appear as a consequence of a high-j - low-j feedback:
On the one hand, the slightly deformed (fp) density aligns the high-j orbitals to form two blades of the shears. On the other hand, the spatial density distributions of these orbitals induce the deformation of the (fp) density.
Regular shears bands appear only if this feedback is strong enough. If fewer high-j orbitals are involved or the low-j orbitals are less polarizable, the sequence of the M1 transitions becomes less regular. The regular shears bands and the irregular multiplets are the two limits of a variety of more or less regular M1 sequences.

As seen in Figs. 9 and 10, the states of the bands are connected by strong M1 and very weak E2 transitions, what are the salient features of the shears bands. This reflects the fact that we consider cases when the number of open shell particles is small, such that the system is still far from the transition to

well deformed shapes and the induced deformations remain fairly small.

5 Relation to the TAC mean - field calculations

The shears bands have first been described by means of the TAC theory [6]. It is a cranking mean - field description based on a Pairing + QQ-interaction allowing for rotation about an arbitrary axis. In this model the dependence of the energy on the relative orientation of the stretched proton and neutron high-j configurations (blades of the shears) originates from their interaction with the deformed potential. This deformed potential is induced by the torus and dumb-bell like density distributions of the high-j orbitals. Thus, the TAC model includes the feedback between the low and high-j particles that turned out to be crucial for the appearance of the bands. Describing the polarization, the TAC is superior to the shell model, because there is no restriction of the configuration space. In the TAC calculations deformations of $0.05 < \beta < 0.10$ and $\gamma \approx -70^{\circ}$ are found [3], i. e. the shape is slightly oblate - triaxial. On the other hand, in TAC the high-j protons and neutrons interact via the deformed field exclusively, whereas in the shell model there is also a direct residual interaction.

In contrast to the shell model, the total angular momentum is treated as a classical vector in TAC. This does not lead to problems as long as one describes regular bands, but multiplet structures are not expected to be well accounted for. The successful quantitative description of the regular shears bands by means of the TAC seems to indicate a dominating role of the polarization mechanism. The description of the transition from multiplets to regular shears bands remains beyond the realm of the TAC mean - field theory, because the direct interaction between the high-j orbitals as well as the quantization of the total angular momentum become important.

6 Comparison with the experiment

In Fig. 8 the calculated level spacings of the $\pi(s_{1/2}^{-2}h_{9/2}i_{13/2})_{11}-\otimes\nu[(i_{13/2}^{-2})(fp)^{-7}]$ configuration are shown together with the transition energies of band 2 in ^{199}Pb [3] to which this configuration is assigned. Obviously, the calculated slope (the $\mathcal{J}^{(2)}$ moment of inertia) is too large and there is a slight kink that is not seen in experiment. These discrepancies may be explained by the restricted configuration space and the corresponding limitation of the included correlations. Inspecting the Nilsson diagrams (cf. e. g. [17]), one realizes that for a deformation of $0.05 < \beta < 0.10$, as found in the TAC calculations, the interaction of the $s_{1/2}$ proton holes with the other states of the $N = 4$ shell is

substantial (upbending of the [400 1/2] level). Thus, the scattering of the two proton holes into the 1d single-particle states should be taken into account. This inclusion of low-j protons is expected to increase the polarizability of the low-j core. It will make the band more regular and increase the coupling between the high-j protons and high-j neutron holes. More energy will be needed to gradually align the two blades of the shears resulting in a lower slope of the curve $J(\omega)$.

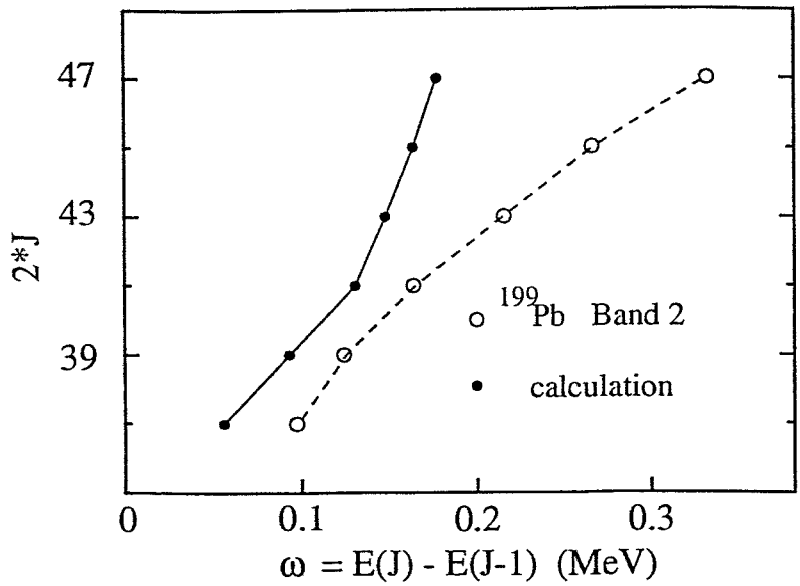

Fig. 8. Comparison of the calculated and experimental transition energies between states with $35/2^+ \leq J^\pi \leq 47/2^+$ of the $\pi(s_{1/2}^{-2}h_{9/2}i_{13/2})_{11^-} \otimes \nu[(i_{13/2}^{-2})(p_{1/2}p_{3/2}f_{5/2})^{-7}]$ configuration. The experimental values are taken from [3].

Fig. 9 shows the reduced probabilities of magnetic dipole transitions calculated for the transitions depicted in Fig. 6. The shell model predicts very fast M1 transitions, which are comparable to the experimental ones [7,4,8]. For the regular shears bands the B(M1) values decrease with increasing spin (Fig. 9a). This behavior has been explained in Ref. [6]: The spin grows by the reorientation of the proton and neutron spin into the direction of the total angular momentum. As a consequence, the transversal component of the magnetic moment decreases along the band leading to smaller M1 transition rates. This predicted decrease of the B(M1) values has been found in Ref. [7]. For the irregular sequences with a full or empty (fp) shell the calculated B(M1) values tend to increase with spin (compare Fig. 6 and 9).

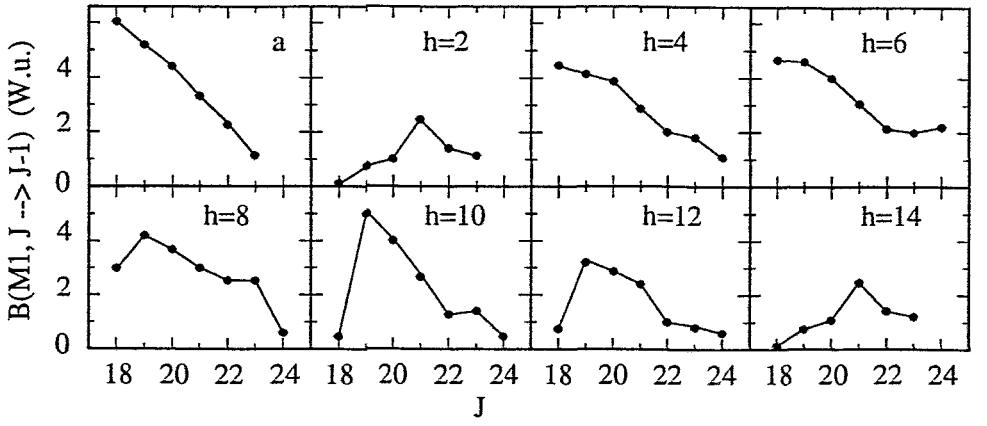

Fig. 9. Calculated $B(\mathrm{M1}, J \to J-1)$ values for $18^- \leq J^\pi \leq 24^-$. In the calculation the coupling of the proton $(s^{-2}_{1/2}h_{9/2}i_{13/2})_{11^-}$ excitation to the neutron configurations $(i_{13/2})^{-2}_{12^+}$ (a) and $(i_{13/2})^{-n}(p_{1/2}p_{3/2}f_{5/2})^{-m}$ (n=0,2; m even; $h = m+n$ denotes the total number of neutron holes) has been considered. The $B(\mathrm{M1})$ values are given in Weisskopf units.

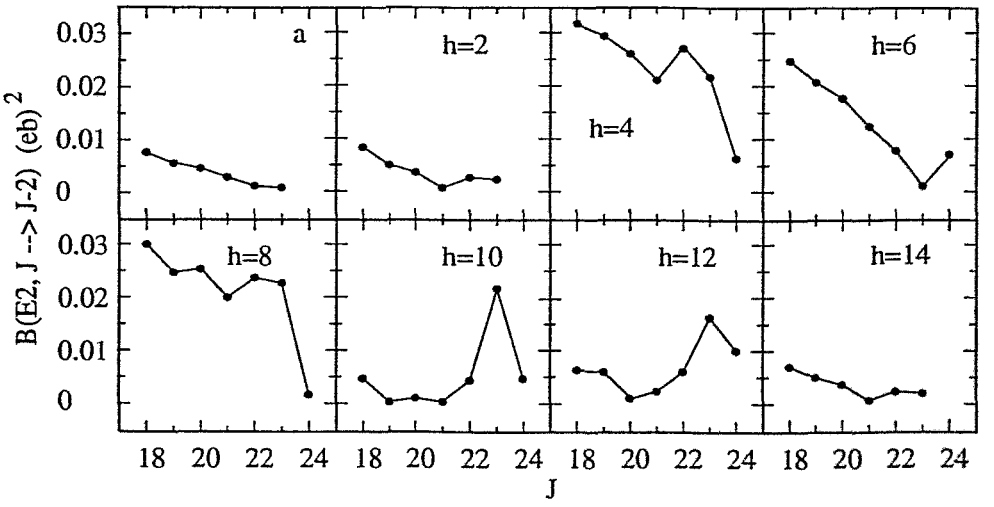

Fig. 10. Calculated $B(\mathrm{E2}, J \to J-2)$ values for $18^- \leq J^\pi \leq 24^-$. In the calculation the coupling of the proton $(s^{-2}_{1/2}h_{9/2}i_{13/2})_{11^-}$ excitation to the neutron configurations $(i_{13/2})^{-2}_{12^+}$ (a) and $(i_{13/2})^{-n}(p_{1/2}p_{3/2}f_{5/2})^{-m}$ (n=0,2; m even; $h = m+n$ denotes the total number of neutron holes) has been considered. The $B(\mathrm{E2})$ values are given in $(eb)^2$.

Experimentally, the $B(\mathrm{E2})$ values for the few observed crossover transitions are in the order of 0.1 to 0.2 $(eb)^2$ [5,7]. The calculated values are about one order of magnitude smaller (cf. Fig. 10). The discrepancy is likely to be

caused by the truncation of the configuration space as well. An expansion of the configuration space by low-spin proton (e.g., $1d_{3/2}$) as well as neutron (e.g., $1f_{7/2}$) orbitals would include more correlations increasing the quadrupole coherence. As discussed above, the fact that the experimental shears bands are more regular than in our calculations seems also to be a consequence of the truncation in our model.

7 Conclusions

We have carried out shell-model calculations in a restricted configuration space of the neutron configurations $[(p_{1/2}p_{3/2}f_{5/2})^{-m}(i_{13/2})^{-n}]$ with $m = 0, ..., 12$ and $n = 0, 1, 2$ coupled to the proton configuration $(s_{1/2}^{-2}h_{9/2}i_{13/2})_{11}$. These calculations give *regular rotational bands* if the (fp) space is approximately half filled ($m = 3, 4, 5, 6, 7$). The bands have the characteristics of the experimental shears bands observed in this region: They start at $J = 16$, have large M1 and very weak E2 transitions. The calculated shears bands terminate for $J = 23$, where protons and neutrons are fully aligned. The calculated bands are somewhat less regular than the experimental ones and have too small $B(E2)$ values. The discrepancies are probably a consequence of our too restricted configuration space.

The appearance of regular rotational bands in such a restricted configuration space is quite remarkable, since the description of rotational bands by the shell model usually operates with much larger configuration spaces. It is the manifestation of a new kind of rotation, different from the familiar rotation of deformed nuclei. As discussed in Ref. [12], this *magnetic rotation* appears as the consequence of the breaking of the intrinsic rotational symmetry by a large magnetic dipole instead of the familiar breaking by an electric quadrupole (deformation). The dipole is generated by few high-j protons and high-j neutron holes. A sufficient quadrupole polarizability and sufficiently many high-j protons and high-j neutron holes (the role of protons and neutrons may be exchanged) are prerequisites of regular bands. Then a feedback mechanism becomes active: The high-j protons and neutron holes induce a slight deformation which acts as a guiding field that aligns the angular momenta of the high-j protons to one angular momentum vector and the angular momenta of the neutron holes to another angular momentum vector. The two angular momentum vectors align gradually with the total angular momentum, forming the band. If the number of high-j orbitals involved and/or the quadrupole polarizability are too small, dipole sequences appear that are intermediate between regular bands and irregular multiplets.

The picture of shears bands, which has been conceived from the TAC mean - field description, is fully confirmed by the analysis of the shell model wave

functions. For a quantitative description of the shears bands the shell model configuration space must be expanded. Though the numerical effort will be significant, it seems to be within the reach of modern computing technology. In particular for less regular dipole sequences the shell model seems to offer an appropriate interpretation. For regular shears bands the TAC mean - field description remains the preferable alternative, because it keeps the numerical effort low and provides a transparent physical picture.

References

[1] R.M. Clark, R. Wadsworth, E.S. Paul, C.W. Beausang, I. Ali, A. Astier, D.M. Cullen, P.J. Dagnall, P. Fallon, M.J. Joyce, M. Meyer, N. Redon, P.H. Regan, W. Nazarewicz and R. Wyss, Phys. Lett. B275 (1992) 247

[2] G. Baldsiefen, H. Hübel, D. Mehta, B.V. Thirumala Rao, U. Birkental, G. Fröhlingsdorf, M. Neffgen, N. Nenoff, S.C. Pancholi, N. Singh, W. Schmitz, K. Theine, P. Willsau, H. Grawe, J. Heese, H. Kluge, K.H. Maier, M. Schramm, R. Schubart and H.J. Maier, Phys. Lett. B275 (1992) 252

[3] G. Baldsiefen, H. Hübel, W. Korten, D. Mehta, N. Nenoff, B.V. Thirumala Rao, P. Willsau, H. Grawe, J. Heese, H. Kluge, K.H. Maier, R. Schubart, S. Frauendorf and H.J. Maier, Nucl. Phys. A574 (1994) 521

[4] E.F. Moore, M.P. Carpenter, Y. Liang, R.V.F. Janssens, I. Ahmad, I.G. Bearden, P.J. Daly, M.W. Drigert, B. Fornal, U. Garg, Z.W. Grabowski, H.L. Harrington, R.G. Henry, T.L. Khoo, T. Lauritsen, R.H. Mayer, D. Nisius, W. Reviol and M. Sferrazza, Phys. Rev. C51 (1995) 115

[5] R.M. Clark, R. Wadsworth, E.S. Paul, C.W. Beausang, I. Ali, A. Astier, D.M. Cullen, P.J. Dagnall, P. Fallon, M.J. Joyce, M. Meyer, N. Redon, P.H. Regan, J.F. Sharpey–Schafer, W. Nazarewicz and R. Wyss, Nucl. Phys. A562 (1993) 121

[6] S. Frauendorf, Nucl. Phys. A557 (1993) 259c

[7] M. Neffgen, G. Baldsiefen, S. Frauendorf, H. Grawe, J. Heese, H. Hübel, H. Kluge, A. Korichi, W. Korten, H.J. Maier, K.H. Maier, J. Meng, D. Mehta, N. Nenoff, M. Piiparinen, M. Schönhofer, R. Schubart, U.J. van Severen, N. Singh, G. Sletten, B.V. Thirumala Rao and P. Wilssau, Proc. Conf. on Physics on Large γ Ray Detectors, Berkeley, USA 1994 and Nucl. Phys. A, in print; cf. also Physica Scripta, T56 (1995) 44

[8] R.M. Clark, R. Wadsworth, H.R. Andrews, C.W. Beausang, M. Bergstrom, S. Clarke, E. Dragalescu, T. Drake, P.J. Dragnall, A. Galindo–Urban, G. Hackman, K. Hauschild, I.M. Hibbert, V.P. Janzen, P.M. Jones, R.W. MacLeod, E.S. Paul, D.C. Radford, A. Semple, A. Astier, D.M. Cullen, P.J. Dagnall, P. Fallon, M.J. Joyce, M. Meyer, J.F. Sharpey–Schafer, J. Simpson, D. Ward and G. Zwartz, Phys. Rev. C50 (1994) 84

[9] G. Baldsiefen, P. Maagh, H. Hübel, W. Korten, S. Chmel, M. Neffgen, W. Pohler, H. Grawe, K.H. Maier, K. Spohr, R. Schubart, S. Frauendorf and H. J. Maier Nucl. Phys. A, subm.

[10] G. Winter, J. Döring, F. Dönau and L. Funke, Z. Phys. A334 (1989) 415

[11] R. Schwengner, G. Winter, J. Reif, H. Prade, L. Käubler, R. Wirowski, N. Nicolay, S. Albers, S. Eßer, P. von Brentano and W. Andrejtscheff, Nucl. Phys. A584 (1995) 159

[12] S. Frauendorf, J. Meng, J. Reif, Proc. Conference on Physics from Large γ ray Detector Arrays, Berkeley (1994), Volume 2, p. 52, LBL-35687

[13] D. Zwarts, Comput. Phys. Commun. 38 (1985) 365

[14] T.T.S. Kuo and G.H. Herling, Naval Research Laboratory Report 2258, 1971

[15] P.W.M. Glaudemans, P.J. Brussaard and B.H. Wildenthal, Nucl. Phys. A102 (1967) 593

[16] R.D. Lawson, Theory of the Nuclear Shell Model, (Clarendon Press, Oxford, 1980)

[17] A. Bohr and B.Mottelson, Nuclear Structure II, (Benjamin, 1975)

[18] E. Caurier, A.P. Zuker, A. Poves and G. Martinez-Pinedo, Phys. Rev. C50 (1994) 225